

**Nitrogen-doped carbon nanotubes embedded with nitrogen-doped  
carbon black anchoring Pd nanocrystals to boost ethanol  
electrooxidation**

Shuwen Li<sup>a\*</sup>, Li Wu<sup>a</sup>, Jinjuan Zhao<sup>a</sup>, Ruxia Li<sup>a</sup>, Honglei Yang<sup>a</sup>, Limin Zhao<sup>b</sup>, Ruifa Jin<sup>b\*</sup>

<sup>a</sup>State Key Laboratory of Applied Organic Chemistry (SKLAOC), College of Chemistry and Chemical Engineering, Lanzhou University, Lanzhou 730000, P. R. China

<sup>b</sup>Inner Mongolia Key Laboratory of Photoelectric Functional Materials, College of Chemistry and Life Sciences, Chifeng University, Chifeng 024000, P. R. China

\*Corresponding authors

E-mail addresses: lishw@lzu.edu.cn (Shuwen Li); Ruifajin@163.com (Ruifa Jin)

## 1. Tables

**Table S1** The N and Pd contents of as-prepared catalysts.

Catalysts	N contents (wt.%)	Pd contents (wt.%)
Pd/NCB	2.17	12.57
Pd/NCNTs	5.69	13.47
Pd/NCB@NCNTs-1	4.91	13.55
Pd/NCB@NCNTs-2	4.80	13.74
Pd/NCB@NCNTs-3	4.13	14.08

**Table S2** N analysis of the catalysts by XPS.

Samples	Pyridinic N		Pyrrolic N		Graphitic N	
	<sup>a</sup> BEs/eV	AP%	<sup>a</sup> BEs/eV	AP%	<sup>a</sup> BEs/eV	AP%
Pd/NCB	398.8	28.8	399.9	61.2	401.3	10.0
Pd/NCNTs	399.1	29.6	400.1	60.3	401.2	10.1
Pd/NCB@NCNTs-2	398.8	27.8	400.0	62.5	401.5	9.7

<sup>a</sup>BEs is binding energy.

**Table S3** Pd 3d analysis of as-prepared catalysts by XPS.

Samples	<sup>a</sup> BEs (eV) Pd(0)		<sup>a</sup> BEs (eV) PdO <sub>x</sub>	
	Pd 3d <sub>5/2</sub>	Pd 3d <sub>3/2</sub>	Pd 3d <sub>5/2</sub>	Pd 3d <sub>3/2</sub>
Pd/CNTs	335.5	340.7	337.6	342.7
Pd/NCB	335.6	340.8	337.8	343.0
Pd/NCNTs	335.6	340.8	337.9	343.0
Pd/NCB@NCNTs-2	335.7	340.9	337.9	343.1

<sup>a</sup>BEs is the binding energy.

**Table S4** Parameters obtained from CV curves.

Catalysts	$S_{\text{ECSA}}$ (m <sup>2</sup> g <sup>-1</sup> )	$j'_f$ (mA cm <sup>-2</sup> )	$j_f$ (mA mg <sup>-1</sup> )	$j_s$ (mA mg <sup>-1</sup> )	Retention ratio (%)
Pd/C	21.2	2.43	515.8	3.5	9.6
Pd/NCB	29.8	3.33	992.2	8.1	21.3
Pd/NCNTs	30.3	3.86	1169.2	11.5	28.1
Pd/NCB@NCNTs-1	34.5	4.11	1412.8	22.3	37.3
Pd/NCB@NCNTs-2	40.4	4.65	1879.3	35.3	43.3
Pd/NCB@NCNTs-3	33.4	4.07	1206.4	18.5	32.7

**Table S5** Parameters obtained from LSV and CO stripping curves.

Catalysts	Tafel slope (mV dec <sup>-1</sup> )	$E_{onset}^{CO}$ (V vs Hg/HgO)	$E_{oxidation}^{CO}$ (V vs Hg/HgO)
Pd/C	243	-0.124	-0.064
Pd/NCB	176	-0.127	-0.069
Pd/NCNTs	157	-0.140	-0.067
Pd/NCB@NCNTs-1	142	-0.156	-0.093
Pd/NCB@NCNTs-2	123	-0.166	-0.106
Pd/NCB@NCNTs-3	154	-0.146	-0.087

**Table S6** Comparison of the electrocatalytic activity of this work with recent reports<sup>1-9</sup>.

Catalysts	$j_f$ (mA mg <sup>-1</sup> ) <sup>a</sup>	Reference
Pd/NCB@NCNTs-2	1879.3	This work
Au@Pd/PdO <sub>x</sub> -35.2	1290.0	1
PdSP metallene	1520.0	2
PdSm NCs/C	1032.7	3
Pd@N,P,S-3DG	1784.1	4
Pd/B-N-Ti <sub>3</sub> C	937.2	5
Pd NPs@Ni SAC	1093.0	6
Pd-Te-2	1203.0	7
Au@PdAu CNCs/C	863.0	8
Pd <sub>0.5</sub> Cu <sub>0.5</sub>	414.3	9

<sup>a</sup>The electrochemical parameters was acquired in 1.0 M KOH and 1.0 M C<sub>2</sub>H<sub>5</sub>OH solution at a scan rate of 50 mV s<sup>-1</sup>.

## 2. Figures

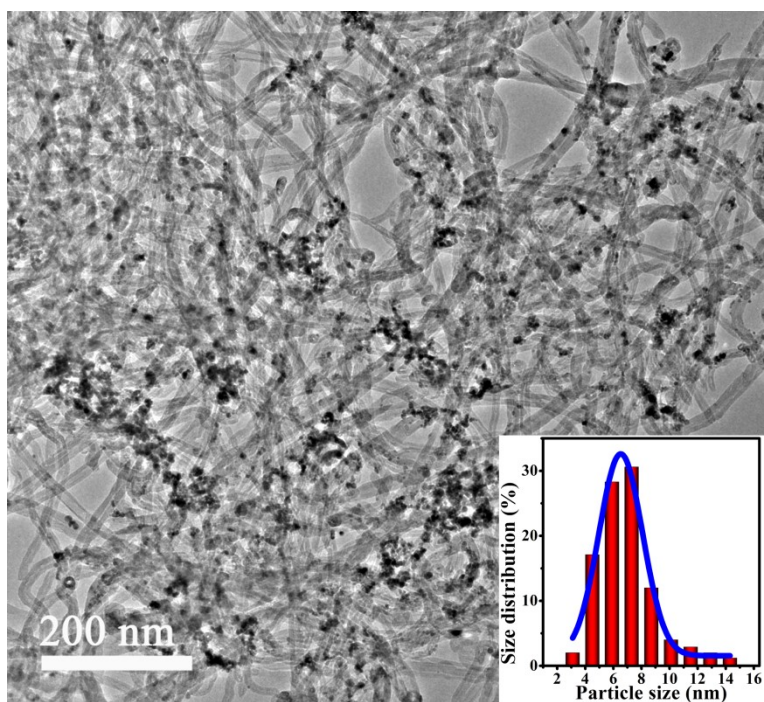


**Figure S1** TEM image of Pd/CNTs.

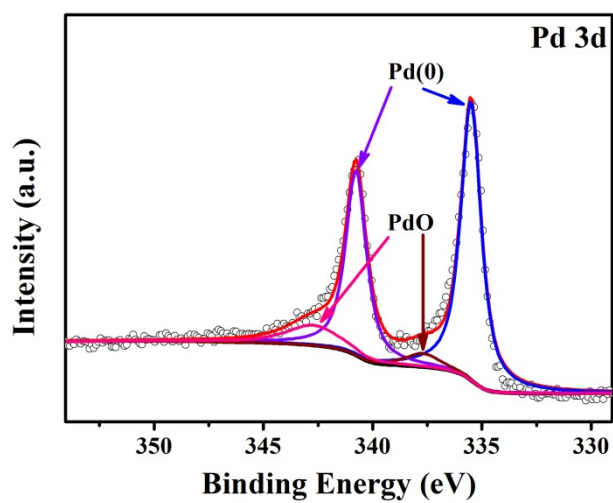


**Figure S2** High-resolution XPS spectrum of Pd 3d for Pd/CNTs (the preparation of Pd/CNTs samples of has been synthesized by a similar process to Pd/NCB@NCNTs).

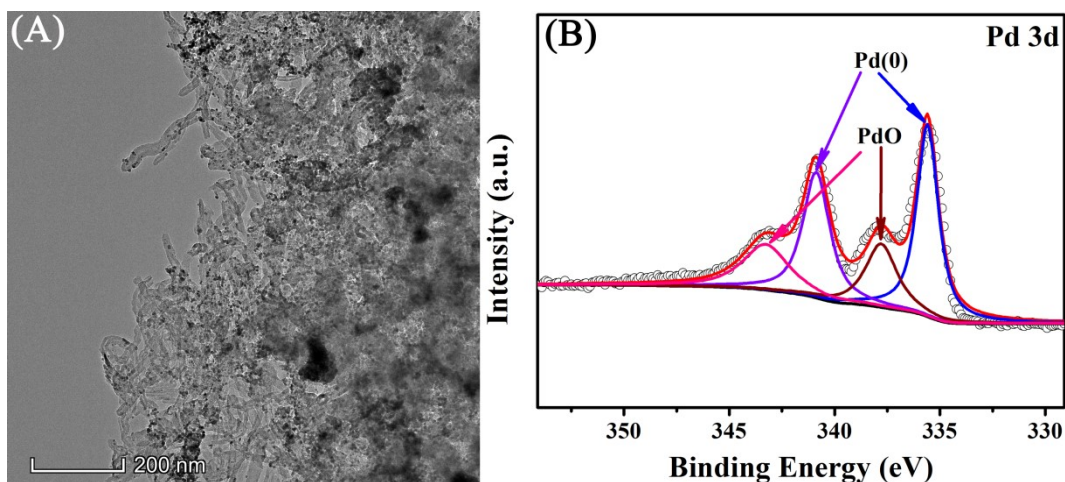


**Figure S3** (A) TEM image and (B) high-resolution XPS spectrum of Pd 3d for Pd/NCB@NCNTs-2 after 500 cycles CV scans.

The morphology of the Pd/NCB@NCNTs-2 after the stability test was examined by TEM and XPS. As displayed in Figure S3A, small amounts of NPs are slightly agglomerated possible due to electrochemical Ostwald ripening, indicating the Pd/NCB@NCNTs-2 catalyst was not basically damaged after 500 cycles CV test. In addition, the Pd contents of Pd/NCB@NCNTs-2 before and after EOR and the stability tests were measured by ICP-OES. The results revealed that the Pd was nearly no lost. Furthermore, the very slightly changes have taken place in the composition, binding energy and chemical state of Pd after 500 cycles CV test (Figure S3B). Therefore, Pd would not be dissolved out after EOR test or the stability test and the Pd/NCB@NCNTs-2 possesses strong stability.

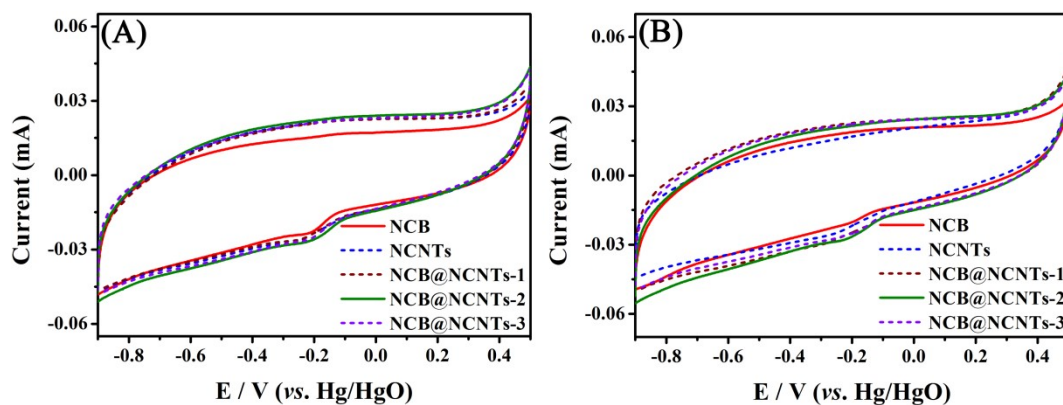
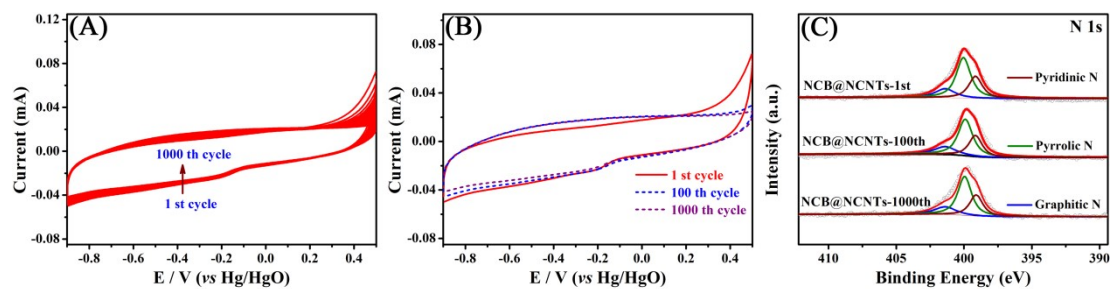


**Figure S4** CVs of the prepared-supports (NCB, NCNTs, NCB@NCNTs-1, NCB@NCNTs-2 and NCB@NCNTs-3) in  $N_2$ -saturated 1.0 M KOH electrolyte (A) and  $N_2$ -saturated 1.0 M KOH and 1.0 M  $C_2H_5OH$  (B) at a sweep rate of  $50 \text{ mV s}^{-1}$ .

The electrocatalytic performance of supports without Pd NCs have been added to demonstrate the roles of Pd and supports. Different from the prepared-catalysts, there are no obvious anodic oxidation peaks for all the prepared-supports (NCB, NCNTs, NCB@NCNTs-1, NCB@NCNTs-2 and NCB@NCNTs-3) as shown in Figure S4, indicating the Pd NCs are catalytic active sites and the NCB, NCNTs, NCB@NCNTs-1, NCB@NCNTs-2 and NCB@NCNTs-3 are carrier materials to stabilize and immobilize Pd NCs.



(D) C and N analysis of NCB@NCNTs-2 by CHN and XPS over CV cycles.

Samples	C contents		N contents		Pyridinic N		Pyrrolic N		Graphitic N	
	wt. %	wt. %	wt. %	wt. %	<sup>a</sup> BEs/eV	AP%	<sup>a</sup> BEs/eV	AP%	<sup>a</sup> BEs/eV	AP%
NCB@NCNTs-2-1st	87.78	5.61	399.2	28.1	400.0	55.1	401.4	16.8		
NCB@NCNTs-2-100th	87.48	5.50	399.1	28.6	399.9	54.4	401.4	17.0		
NCB@NCNTs-2-1000th	87.35	5.48	399.1	28.7	399.9	54.2	401.4	17.1		

<sup>a</sup>BEs is binding energy.

**Figure S5** CVs of NCB@NCNTs-2 from 1st to 1000th cycle in N<sub>2</sub>-saturated 1.0 M KOH and 1.0 M C<sub>2</sub>H<sub>5</sub>OH (A, B) at a sweep rate of 50 mV s<sup>-1</sup>. (C) High-resolution XPS spectra of N 1s for NCB@NCNTs-2 over 1st, 100th and 1000th. (D) C and N analysis of NCB@NCNTs-2 by CHN and XPS over CV cycles.

The electrochemical stability of the NCB@NCNTs-2 was conducted through continuous CV cycles in N<sub>2</sub>-saturated 1.0 M KOH solution containing 1.0 M ethanol (Figure S5A-S5B). As shown in Figure S5A-5B, the shape and capacitance of NCB@NCNTs-2 have undergone some changes from 1st to 100th cycles, which possibly is ascribed to a structural or surface reorganization of NCB@NCNTs-2. The shape and capacitance of NCB@NCNTs-2 occur tiny changes 100th to 1000th cycles mainly by loss of a small amount volume and collapse, illustrating the NCB@NCNTs-2 possesses high electrochemical stability. As reported, the noble metal nanoparticles grow mainly by Ostwald ripening mimicking under normal operation, while the carbon support is stable. Therefore, the carbon support degrades mainly by loss of a small amount volume and collapse, which is in consistence with the results of continuous CV cycles. Moreover, the elemental composition and chemical state of the NCB@NCNTs-2 over CV cycles was analyzed by elemental composition analysis and XPS spectra. As shown in Figure S5C and S5D, the N

contents for NCB@NCNTs-2 is slightly reduced from 1st to 100th cycles and almost is not change from 100th to 1000th cycles. Furthermore, the types of N almost is not change from 100th to 1000th cycles. The above facts indicate that the NCB@NCNTs-2 possesses high stability during EOR.

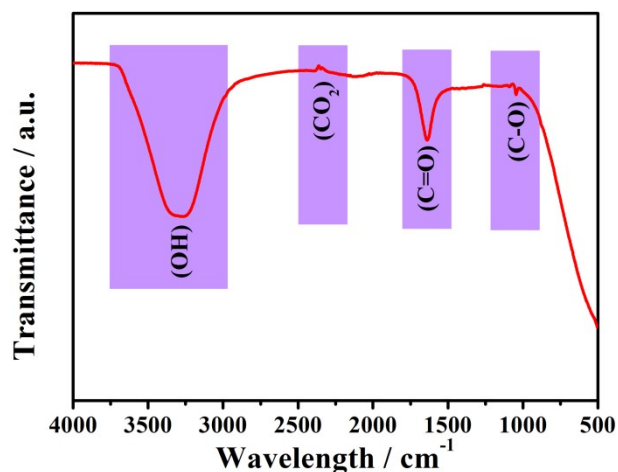


**Figure S6** FTIR of EOR products for Pd/NCB@NCNTs-2.

Figure S6 shows the FTIR of EOR products for Pd/NCB@NCNTs-2. The presence of peaks at 3290, 1637, 1045 and 2349  $\text{cm}^{-1}$  are assigned to ( $\text{OH}_{\text{acid}}$ ), ( $\text{C}=\text{O}_{\text{acid}}$ ), ( $\text{C}-\text{O}_{\text{acid}}$ ) and ( $\text{CO}_2$ ), respectively<sup>10-12</sup>. The distinct FTIR spectra of the EOR products manifests that the acetic acid is primary product for Pd/NCB@NCNTs-2.



## References

1. J. Hao, B. Liu, M. Takahashi, S. Maenosono and J. Yang, *Catal. Sci. Technol.*, 2023, **13**, 4141-4147.
2. H. Wang, Y. Guo, Q. Mao, H. Yu, K. Deng, Z. Wang, X. Li, Y. Xu and L. Wang, *Nanoscale*, 2023, **15**, 7765-7771.
3. G. Zhang, Y. Wang, Y. Ma, Y. Zheng, H. Zhang, M. Tang and Y. Dai, *Catal. Today*, 2023, **409**, 63-70.
4. C. Karaman, *Int. J. Hydrogen Energy*, 2023, **48**, 6691-6701.
5. Z. Chen, J. Cao, X. Wu, D. Cai, M. Luo, S. Xing, X. Wen, Y. Chen, Y. Jin, D. Chen, Y. Cao, L. Wang, X. Xiong and B. Yu, *ACS Appl. Mater. Inter.*, 2022, **14**, 12223-12233.
6. S. Li, A. Guan, H. Wang, Y. Yan, H. Huang, C. Jing, L. Zhang, L. Zhang and G. Zheng, *J. Mater. Chem. A*, 2022, **10**, 6129-6133.
7. Q. Zhang, K. Wang, M. Zhang, T. Chen, L. Li, S. Shi and R. Jiang, *CrystEngComm*, 2022, **24**, 5580-5587.
8. G. Zhang, Y. Ma, X. Fu, W. Zhao, F. Liu, M. Liu and Y. Zheng, *CrystEngComm*, 2021, **23**, 2582-2589.
9. P. C. Ashly, S. Sarkar, S. C. Sarma, K. Kaur, U. K. Gautam and S. C. Peter, *J. Power Sources*, 2021, **506**, 230168.
10. A. K. Ipadeola, A. Abdelgawad, B. Salah, A. M. Abdullah and K. Eid, *Langmuir*, 2023, **39**, 13830-13840.
11. A. Bach Delpeuch, F. Maillard, M. Chatenet, P. Soudant and C. Cremers, *Appl. Catal. B-Environ.*, 2016, **181**, 672-680.
12. X. H. Xia, H. D. Liess and T. Iwasita, *J. Electroanal. Chem.*, 1997, **437**, 233-240.